

Atomic and Nuclear Physics

Atomic Shell



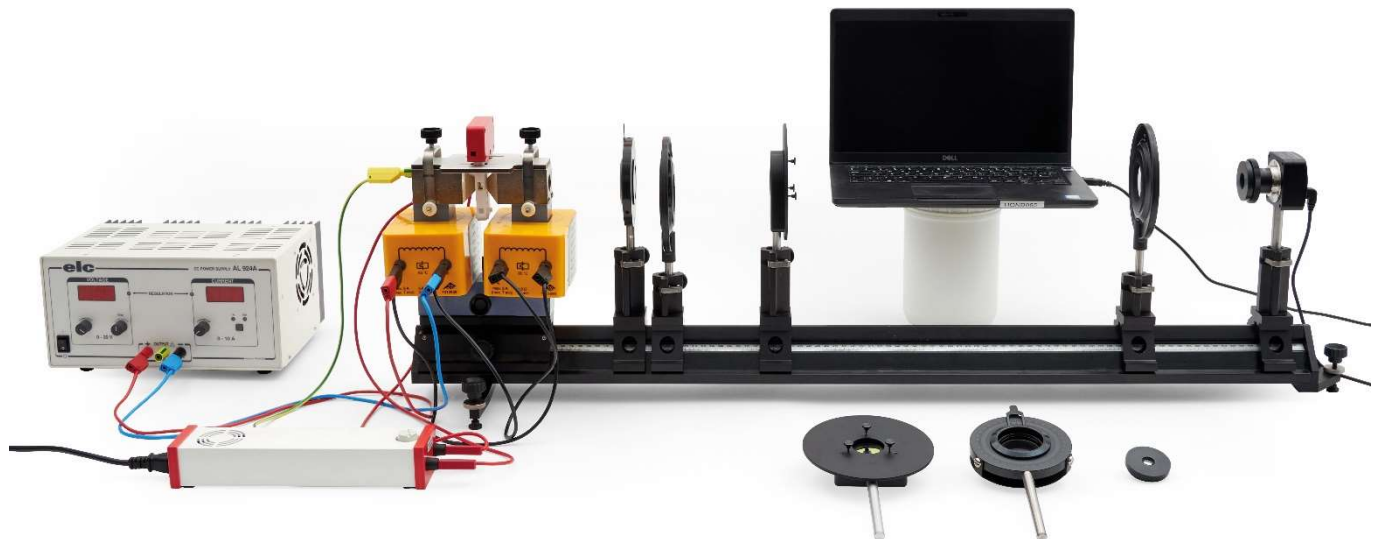
Normal and anomalous Zeeman Effect, Hyperfine Structure, Fabry-Pérot Interferometer and Bohr Magneton

INVESTIGATION OF THE NORMAL AND ANOMALOUS ZEEMAN-EFFECT IN LONGITUDINAL AND TRANSVERSAL CONFIGURATION, OBSERVATION OF THE HYPERFINE STRUCTURE, SPECTROSCOPY WITH A FABRY-PÉROT ETALON AND DETERMINATION OF THE BOHR MAGNETON

- Observation of doublet and triplet splitting of the red cadmium line in an external magnetic field
- Investigation of the polarisation of the doublet and triplet components
- Observation of the hyperfine structure
- Observation of quartet and sextet splitting of the turquoise Cadmium line in an external magnetic field
- Investigation of the polarisation of the quartet and sextet components
- Experimental introduction to the Fabry-Pérot interferometer using the example of the normal Zeeman effect
- Measuring the interference rings of the Fabry-Pérot etalon as a function of the external magnetic field
- Determination of the Bohr Magneton

UE5020800

09/24 TL/UD



Normal Zeeman Effect

INVESTIGATION OF THE NORMAL ZEEMAN EFFECT IN LONGITUDINAL UND TRANSVERSAL CONFIGURATION

- Observation of doublet and triplet splitting of the red cadmium line in an external magnetic field.
- Investigation of the polarization of the doublet and triplet components.

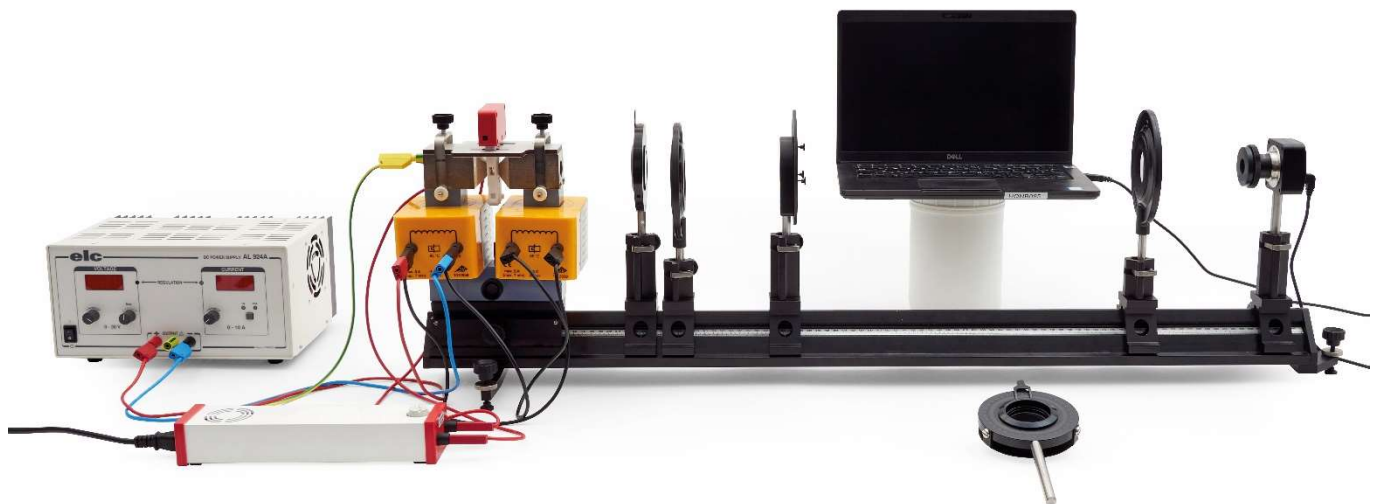


Fig. 1: Experimental setup for the normal Zeeman effect in longitudinal configuration

GENERAL PRINCIPLES

The Zeeman effect refers to the splitting of atomic energy levels or spectral lines under the influence of an external magnetic field. It was discovered in 1896 by its namesake Pieter Zeeman as a broadening of the sodium D lines and classically explained by Hendrik Antoon Lorentz with the help of the Lorentz force, which the magnetic field exerts on the electrons in the atomic shell. In this so-called normal Zeeman effect, as is the case for the red cadmium line ($\lambda = 643.8 \text{ nm}$), for example, a double splitting into a line doublet is observed parallel to the magnetic field (longitudinal) and a triple splitting into a line triplet is observed perpendicular to the magnetic field (transversal). More complex splittings are referred to as the anomalous Zeeman effect, which could only be explained with the help of the existence of the electron spin postulated by Goudsmit and Uhlenbeck in 1925. Quantum mechanically, the anomalous Zeeman effect is based on the interaction of the magnetic field with the magnetic moment of the electron shell generated by the orbital angular momentum and spin of

the electrons. In this respect, the anomalous Zeeman effect represents the normal case, the normal Zeeman effect a special case.

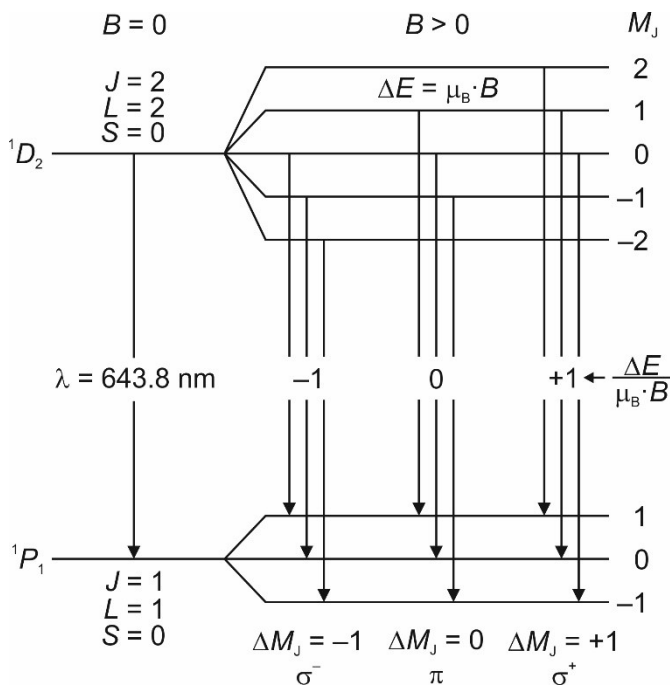


Fig. 2: Normal Zeeman effect at the red cadmium spectral line. Splitting of the energy levels and transitions permitted according to the selection rules for electric dipole radiation

The normal Zeeman effect only occurs for transitions between atomic states whose total spin adds up to $S = 0$. The red Cd line corresponds to the transition $^1D_2 \rightarrow ^1P_1$ with the wavelength $\lambda = 643.8 \text{ nm}$ (Fig. 2). Since both levels have a total spin with the quantum number $S = 0$, the normal Zeeman effect can be observed here, and the total angular momentum $\mathbf{J} = \mathbf{L} + \mathbf{S}$ corresponds to the total orbital angular momentum, i.e. $\mathbf{J} = \mathbf{L}$. It generates a magnetic moment

$$(1) \quad \boldsymbol{\mu} = \frac{\mu_B}{\hbar} \cdot \mathbf{J}$$

with the Bohr magneton

$$(2) \quad \mu_B = \frac{e}{2 \cdot m_e} \cdot \hbar = 9.274 \cdot 10^{-24} \frac{\text{J}}{\text{T}}$$

e : elementary charge

m_e : mass of the electron

$\hbar = h/2\pi$: reduced Planck constant

In an external magnetic field

$$(3) \quad \mathbf{B} = \begin{pmatrix} 0 \\ 0 \\ B \end{pmatrix}$$

the energy

$$(4) \quad E = \boldsymbol{\mu} \cdot \mathbf{B} = \mu_z \cdot B$$

is associated with the magnetic moment. Due to the directional quantization, the component J_z of the total angular momentum parallel to the magnetic field can only have the values

$$(5) \quad J_z = M_J \cdot \hbar \text{ mit } M_J = -J, -(J-1), \dots, (J-1), J.$$

J : Total angular momentum quantum number

The energy level with the total angular momentum quantum number J thus splits into $2J+1$ equidistant components, which differ in the magnetic quantum number M_J (Fig. 2). With Eq. (1) follows

$$(6) \quad \mu_z = \frac{\mu_B}{\hbar} \cdot J_z,$$

thus, according to Eq. (4)

$$(7) \quad E = \mu_z \cdot B = \frac{\mu_B}{\hbar} \cdot J_z \cdot B$$

and finally with Eq. (5):

$$(8) \quad E = \mu_B \cdot M_J \cdot B.$$

The energy distance between two levels with energies E_1 and E_2 ($E_1 > E_2$) is therefore calculated as follows:

$$(9) \quad \Delta E = E_1 - E_2 = (M_{J,1} - M_{J,2}) \cdot \mu_B \cdot B = \Delta M_J \cdot \mu_B \cdot B.$$

According to Eq. (5), level 1D_2 is split into five and level 1P_1 into three components, each with the equidistant energy difference given by Eq. (9).

According to the selection rules for electric dipole radiation, transitions between these levels are permitted with

$$(10) \quad \Delta M_J = \begin{cases} +1 & \text{(right circularly polarized light, } \sigma^+) \\ 0 & \text{(linearly polarized light, } \pi) \\ -1 & \text{(left circularly polarized light, } \sigma^-) \end{cases},$$

where the emitted light is polarized as indicated above. Since three of the nine theoretically possible transitions coincide in terms of energy, a total of three spectral lines can be observed (Fig. 2), one unshifted π component and, according to $E = \hbar \cdot \omega$ two σ components shifted by

$$(11) \quad \Delta\lambda = -\frac{\lambda^2}{2 \cdot \pi \cdot \hbar \cdot c} \cdot \Delta E$$

c : vacuum speed of light

with a correspondingly higher or lower wavelength. Eq. (11) results in a shift of $|\Delta\lambda| = 0.0065 \text{ nm}$ by inserting Eq. (9) and (2) for the flux density $B = 334 \text{ mT}$ set in the experiment.

The spatial distribution of the emitted light is different for the π and the two σ components. The case $\Delta M_J = 0$ classically corresponds to a Hertzian dipole oscillating parallel to the magnetic field. Accordingly, linearly polarized light is emitted perpendicular to the magnetic field (transversal) and no light is emitted parallel to the magnetic field (longitudinal) (Fig. 3). The cases $\Delta M_J = \pm 1$ correspond to two dipoles oscillating perpendicular to each other with a phase difference of 90° . Accordingly, light that is circularly polarized parallel to the magnetic field is emitted both parallel and perpendicular to the magnetic field, namely left circularly polarized for $\Delta M_J = -1$ and right circularly polarized for $\Delta M_J = +1$.

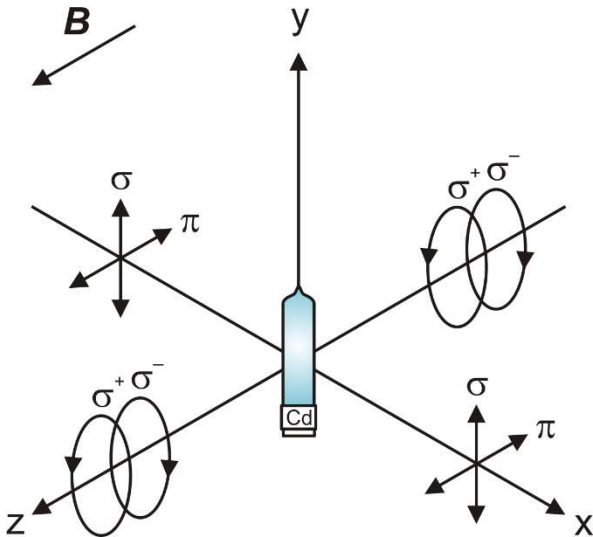


Fig. 3: Polarization of electric dipole radiation depending on the direction of propagation

A quarter-wavelength filter with a downstream polarization filter is therefore required to analyze the polarization of light when observing in the longitudinal direction, as the observation is made perpendicular to the polarization plane of the σ components (Fig. 3). The quarter-wavelength filter converts the circularly polarized light into linearly polarized light, which can then be analyzed using the polarization filter. When the quarter-wavelength filter is set to -45° , the σ^+ component is converted accordingly and can be observed, while the σ^- component disappears. When the quarter-wavelength filter is set to $+45^\circ$, the opposite is true. Only one polarization filter is required for observation in the transverse direction, as the observation is made parallel to the plane of polarization of the σ components, and these appear therefore linearly polarized (Fig. 3). The π component is always linearly polarized. When the polarization filter is set to 0° , the σ components can be observed accordingly, while the π component disappears. When the polarization filter is set to 90° , the opposite is true.

In the experiment, the splitting is observed with the help of a digital camera preceded by a Fabry-Pérot etalon and imaging optics. The Fabry-Pérot etalon is designed to fulfill the resonance condition for the specific wavelength of 643.8 nm of the red Cd line. When the light from the cadmium lamp passes through the Fabry-Pérot etalon, interference rings are created which, like the spectral line, are split as a function of the external magnetic field and imaged onto the camera sensor by the optics. Observation parallel or perpendicular to the external magnetic field is made possible by a rotating electromagnet. The splitting is observed qualitatively and the polarization of the doublet and triplet components is examined using a quarter-wavelength filter with polarization attachment and a polarization filter.

EQUIPMENT LIST

1	Cadmium lamp with accessories @230 V	1021366
or		
1	Cadmium lamp with accessories @115 V	1021747
1	Fabry-Pérot etalon 644 nm	1020903
1	DC power supply, linear regulated, 1 – 30V, 0 – 10A @230V	1025380
or		
1	DC power supply, 0 – 20 V, 0 – 5 A @115 V	1003311
1	U Core D	1000979
2	Coil D, 900 turns	1012859
1	Electromagnet accessory for Zeeman effect	1021365
1	Microscope camera BRESSER MikroCam SP 3.1	1024060
1	Lens 12 mm for Bresser microscope camera	1024059
1	Stainless steel rod with ¼ inch thread, 100 mm	1025431
1	Red filter mounted on holder	1025376
2	Convex lens on stem f =+100 mm	1003023
1	Quarter-wavelength filter on stem	1021353
1	Polarising attachment	1021364
1	Polarisation filter on stem	1008668
1	Optical precision bench D, 1000 mm	1002628
1	Support for optical bench D, set	1012399
1	Optical base D	1009733
3	Optical rider D, 90/36	1012401
2	Optical rider D, 60/36	1002639
1	Safety experiment leads, 75 cm, blue, red, (2 pcs)	1017718
1	Safety experiment leads, 75 cm, black, (2 pcs)	1002849

SAFETY INSTRUCTIONS

- Before setting up the experiment, read and observe the operating instructions for the devices and in particular the safety instructions formulated therein.
- Protect the Cd lamp from mechanical shocks. Do not touch the glass bulb of the Cd lamp with bare hands.
- Only operate the Cd lamp with the ballast supplied. Before putting the Cd lamp mounted on the electromagnet in operation, it is essential to establish the protective earthing. To do this, connect the PE sockets on the ballast and the pole piece of the electromagnet accessory for Zeeman effect (1021365) to each other using the yellow-green safety experiment lead (protective earth conductor) supplied.
- Before putting the electromagnet in operation, ensure that the pole pieces are in the correct position as described in the operating instructions for the electromagnet accessory for Zeeman effect (1021365).

The maximum current through the coils D with 900 turns is 5 A (7 minutes). It can be doubled for short periods (30 seconds). The coils have an internal reversible thermal fuse which trips at a winding temperature of 85°C. The reset time is 10-20 minutes, depending on the ambient temperature.

- Carry out the measurement quickly enough to prevent the thermal fuse from tripping due to high currents flowing for too long.
- Do not operate the coils without a transformer core.

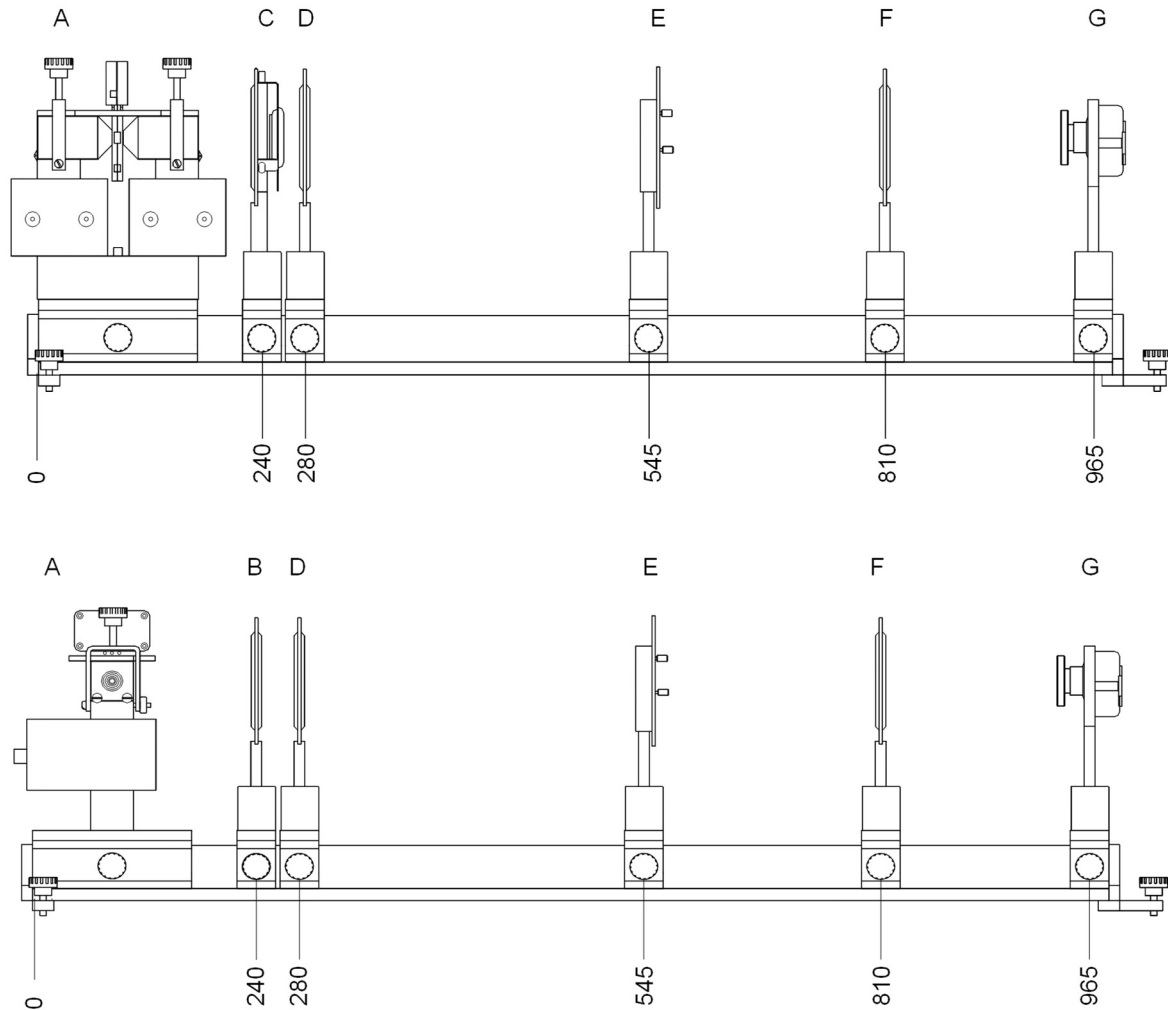


Fig. 4: Experimental setup for the normal Zeeman effect in longitudinal (top) and transversal (bottom) configuration. A: Electromagnet with Cd lamp, B: Polarization filter, C: Quarter wavelength filter with polarizing attachment, D: Convex lens $f = 100$ mm (condenser lens), E: Fabry-Pérot etalon, F: Convex lens $f = 100$ mm (imaging lens), G: Camera with 12 mm lens. See text for exact positioning of components

GENERAL NOTES

The camera software must be installed on the measuring computer.

It is recommended to carry out the experiment in a dark room in order to minimize stray light from the surroundings and to achieve optimum exposure and contrast of the camera's live image.

Due to the temperature sensitivity of Fabry-Pérot etalons, the center of the interference rings may look differently depending on the ambient temperature and may therefore differ from the screenshots in this manual.

SETUP

Mounting the electromagnet and the Cd lamp

- Mount the supports for optical bench (1012399), the long one on the left-hand side of the optical bench, the short one on the right-hand side (scale at the front). Set up the optical bench on a level experimental site.

- Position and fix the optical base (1009733) on the optical bench so that it is flush left with the front plate (Fig. 4).
- Assemble the electromagnet in longitudinal configuration (Fig. 4 top) on the optical base as described in the operating instructions for the electromagnet accessory for Zeeman effect (1021365).
- Mount the cadmium lamp on the electromagnet as described in the operating instructions for the Cd lamp with accessories (1021366 / 1021747).
- Connect the PE sockets on the ballast of the Cd lamp and on the pole piece of the electromagnet using the supplied yellow-green safety experiment lead (protective conductor).
- Connect the Cd lamp to the ballast using the 4 mm safety experiment leads. Connect the ballast to the mains using the mains cable. Do not switch on the ballast yet.

- Connect the “0” tap of the left coil to the “900” tap of the right coil and the “0” tap of the right coil to the “900” tap of the left coil. Then connect the “0” tap of the left coil to the “-” output of the DC power supply unit and the “900” tap of the left coil to the “+” output of the DC power supply unit (Fig. 1). Connect the DC power supply unit to the mains using the mains cable. Do not switch on the DC power supply unit yet.

Mounting the camera and optics

- Screw the tripod rod (1025431) into the 1/4” tripod thread at the bottom of the camera.
- Screw the 12 mm lens (1024059) into the C-mount thread on the front of the camera.
- Screw the red filter (1025376) onto the 12 mm lens.
- Mount the polarizing attachment (1021364) on the quarter-wavelength filter (1021353) as described in the operating instructions.

The polarization filter on stem (1008668), the two convex lenses on stem, $f = 100$ mm (1003023) and the Fabry-Pérot etalon (1020903) require no further assembly.

Starting up the experiment and adjustment

- Switch on the ballast of the Cd lamp and wait approx. 5 minutes.

After a warm-up time of approx. 5 minutes, the Cd lamp has reached 90% of its light output.

- Position and fix a long optical rider (1012401) for the camera on the optical bench so that it is flush right with the front plate. Insert the camera into the optical rider as far as it will go, then move it upwards by approx. 2 cm and fix it.
- Center the 12 mm lens so that it has sufficient clearance in both directions of rotation.
- Position and fix a short optical rider (1002639) for the imaging lens (convex lens $f = 100$ mm, 1003023) at 810 mm. Insert the imaging lens into the optical rider as far as it will go and fix it.
- Start the computer and connect the camera to the computer using the USB cable.
- Start the software. The camera is automatically detected and appears in the camera list. Select the camera and click on it.

The live image is displayed in the window and looks like Fig. 5 after the optimization described below.

- Darken the room if the live image is affected by stray light.

Note:

The screenshots in Fig. 5 - Fig. 7c were taken in a completely darkened room.

- Open the “Power Frequency (anti-flicker)” menu item in the camera window (scroll down if necessary) and click on “AC (50 Hz)” or “AC (60 Hz)”.

This setting minimizes the influence of the mains frequency on the camera’s live image.

- Select the optimum exposure time manually. Do not use the white balance, otherwise the effect of the red filter will be compensated.
- If necessary, optimize the sharpness by turning the 12 mm lens.
- If necessary, move the camera slightly up or down in the optical rider so that the image is centered.

Note:

Due to the optical imaging, a real, upside-down image is created. If the camera is moved upwards in the optical rider, the image moves downwards and vice versa.

- Position and fix a short optical rider (1002639) for the condenser lens (convex lens $f = 100$ mm, 1003023) at 280 mm on the optical bench. Insert the condenser lens into the optical rider as far as it will go and fix it. If necessary, move the imaging lens so that the light spot appears to fill the image and adjust the exposure time (live image as in Fig. 6).
- Position and fix a long optical rider (1012401) for the Fabry-Pérot etalon (1020903) at 545 mm on the optical bench. Insert the Fabry-Pérot etalon into the optical rider as far as it will go and fix it.

Note:

The interference rings may appear blurred and too bright. To optimize sharpness and exposure, the camera position, focus and exposure time have to be adjusted.

- Move the camera to 965 mm, if necessary move it slightly up or down in the optical rider so that the image is centered again, optimize the sharpness by turning the 12 mm lens and adjust the exposure time (live image as in Fig. 7).
- Do not yet place the quarter-wavelength filter with polarizing attachment or the polarization filter in the beam path.

The setup is now configured for the experiment.

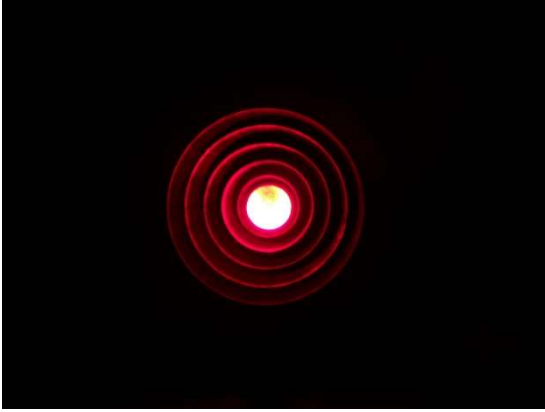


Fig. 5: Live image with camera and imaging lens. Stepped hole of the pole piece and light spot of the Cd lamp appear concentric and centered

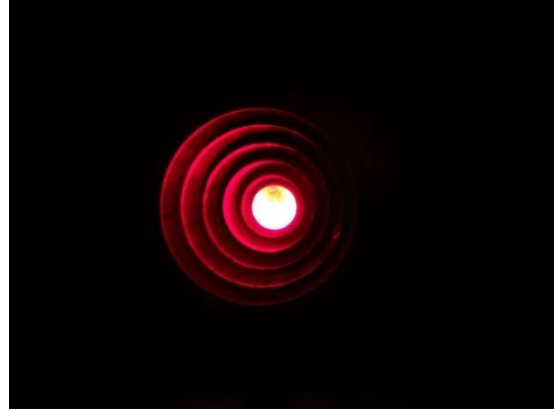


Fig. 5a: Electromagnet twisted. The stepped hole does not appear concentric. Correction: Turn the electromagnet so that it is centered

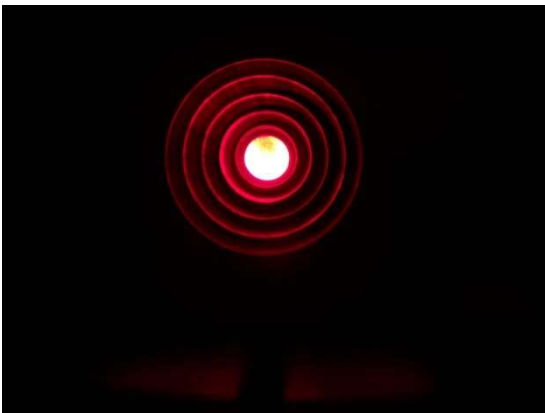


Fig. 5b: Camera too low in the optical rider. Correction: Move the camera up in the optical rider so that it is centered

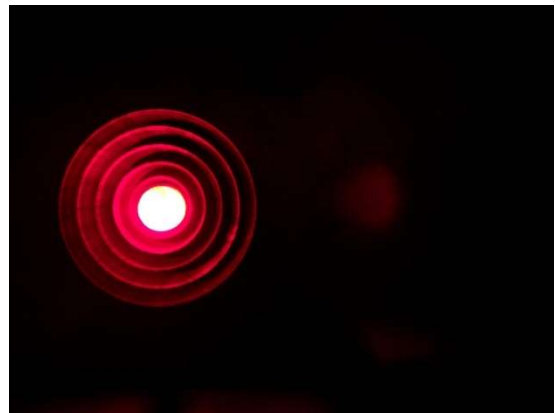


Fig. 5c: Camera twisted in the optical rider. Correction: Rotate the camera in the optical rider so that it is centered

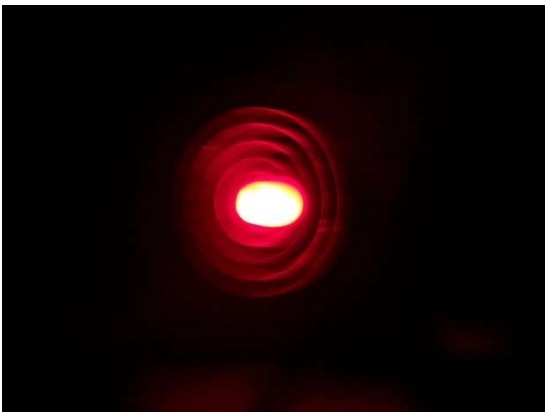


Fig. 5d: Imaging lens twisted in the optical rider. Correction: Rotate the imaging lens in the optical rider so that it is aligned perpendicular to the optical axis



Fig. 6: Live image with condenser lens



Fig. 6a: Condenser lens twisted in the optical rider. Correction: Rotate the condenser lens in the optical rider so that it is aligned perpendicular to the optical axis



Fig. 7: Live image with Fabry-Pérot etalon

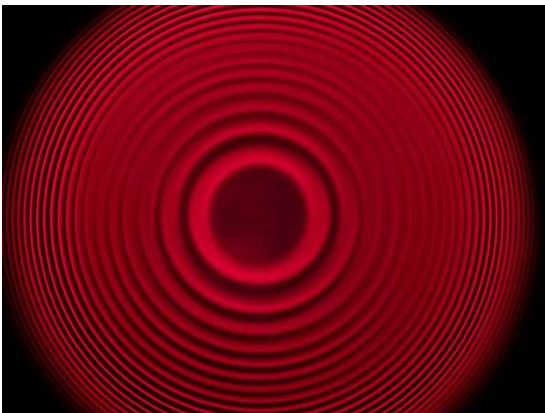


Fig. 7a: Poor focusing. Correction: Turn the 12 mm lens so that the interference rings are clearly visible



Fig. 7b: Etalon twisted in the optical rider. Correction: Rotate the etalon in the optical rider so that it is aligned perpendicular to the optical axis



Fig. 7c: Etalon tilted. Correction: Adjust using the three adjusting screws on the housing.

EXPERIMENT PROCEDURE, MEASUREMENT EXAMPLE AND EVALUATION

Observation in longitudinal direction

Carry out the following steps, observe how the interference rings change and take screenshots (Fig. 8).

- Do not apply an external magnetic field.

Only the interference rings generated by the Fabry-Pérot etalon are observed, each of which corresponds to the red Cd spectral line (Fig. 8a).

- Apply an external magnetic field by switching on the DC power supply unit and increasing the current through the coils to 3.5 A ($B = 334$ mT).

Note:

When a magnetic field is applied, the exposure time should be ≥ 20 ms, as otherwise “flickering lines” may occur due to an interference of the camera’s “rolling shutter sensor”.

The splitting into the line doublet with the two shifted components σ^- and σ^+ is observed, the unshifted π component is not observed (Fig. 8b).

- With the magnetic field applied, position the quarter-wavelength filter with polarization attachment between the electromagnet and the convex lens using a long optical rider (1012401) (Fig. 4 C).

Note:

The quarter-wavelength filter must be on the side of the Cd lamp.

- With the magnetic field applied, set the quarter-wavelength filter with polarization attachment to -45° .

The σ^- component disappears (Fig. 8c).

- With the magnetic field applied, set the quarter-wavelength filter with polarization attachment to $+45^\circ$.

The σ^+ component disappears (Fig. 8d).

- Remove the quarter-wavelength filter with polarization attachment from the beam path.
- Reduce the current to zero and switch off the DC power supply unit.

Observation in transversal direction

- Turn the electromagnet so that the pole pieces are oriented perpendicular to the direction of the optical axis (Fig. 4).
- Do not apply an external magnetic field.

Only the interference rings generated by the Fabry-Pérot etalon are observed, each of which corresponds to the red Cd spectral line (Fig. 8e, Fig. 9).

- Apply an external magnetic field by switching on the DC power supply unit and increasing the current through the coils to 3.5 A ($B = 334$ mT).

The splitting into the line triplet with the unshifted π component and the two shifted components σ^- and σ^+ is observed (Fig. 8f, Fig. 9).

- With the magnetic field applied, position the polarization filter between the electromagnet and the convex lens (Fig. 4 B) and set it to 0° , i.e. perpendicular to the magnetic field.

The π component disappears (Fig. 8g, Fig. 9).

- With the magnetic field applied, set the polarization filter to 90° , i.e. parallel to the magnetic field.

The two σ components disappear (Fig. 8h, Fig. 9).

- Remove the polarization filter from the beam path.
- Reduce the current to zero and switch off the DC power supply unit.

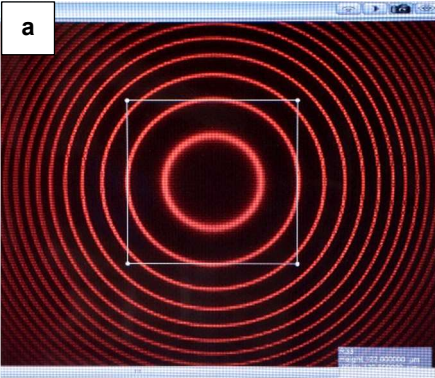
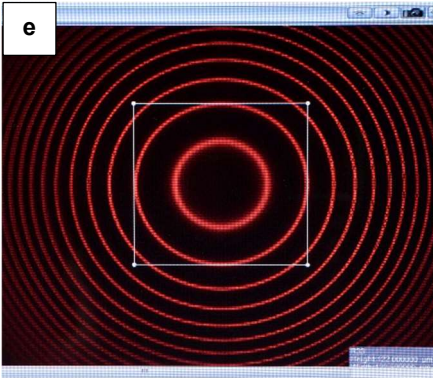
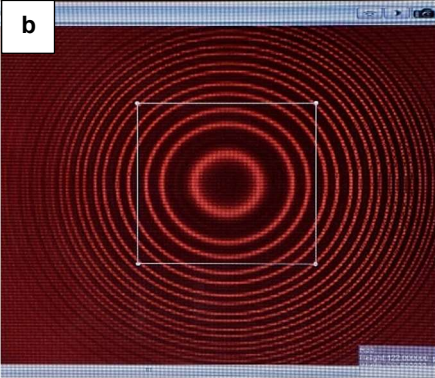
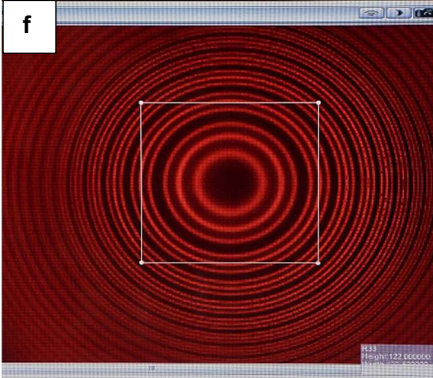
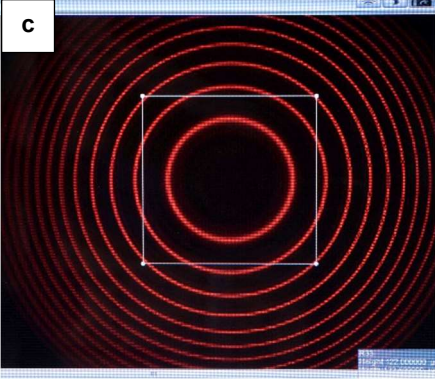
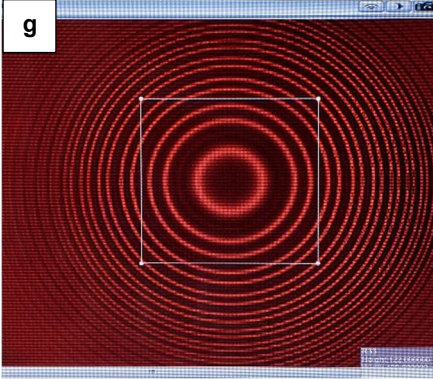
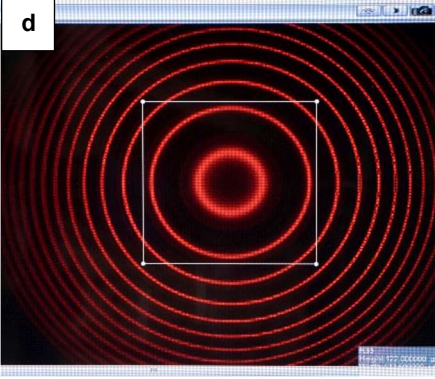
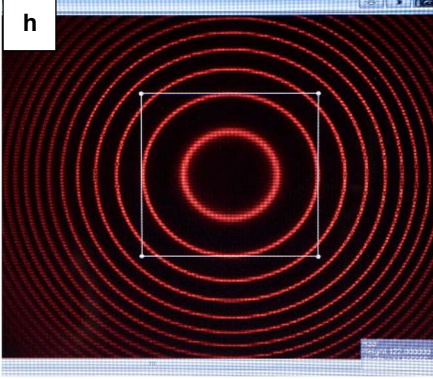
		Longitudinal	Transversal
$B = 0$	Without quarter-wavelength filter & polarization attachment		
	Without quarter-wavelength filter		
$B > 0$	$\lambda/4$ & Pol @ -45°		
	$\lambda/4$ & Pol @ $+45^\circ$		
			Without polarization filter
			Pol $\perp B$ (0°)
			Pol $\parallel B$ (90°)

Fig. 8: Observation of the doublet and triplet splitting of the red cadmium line in the external magnetic field and investigation of the polarization. For better orientation, the second interference ring counted from the center is marked with a frame

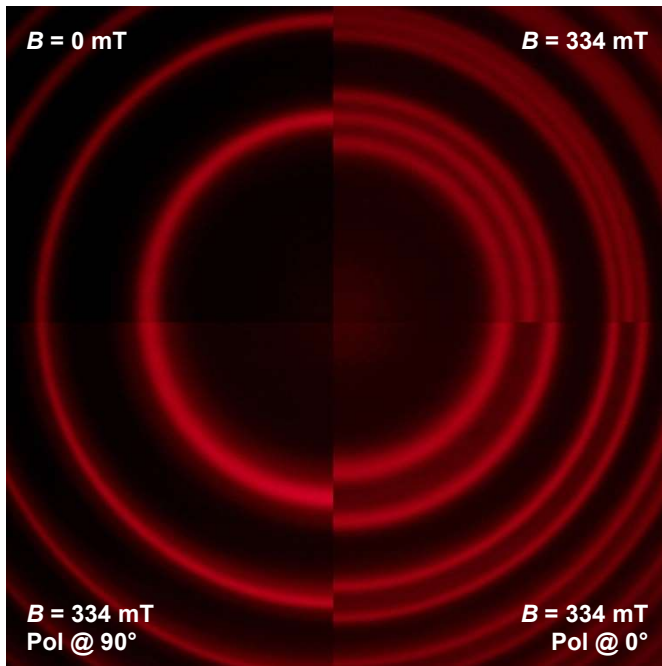


Fig. 9: Normal Zeeman effect when observed in transversal direction. Splitting of the interference rings and polarization states at a glance

Anomalous Zeeman Effect and Hyperfine Structure

INVESTIGATION OF THE ANOMALOUS ZEEMAN EFFECT IN LONGITUDINAL AND TRANSVERSAL CONFIGURATION

- Observation of the hyperfine structure
- Observation of quartet and sextet splitting of the turquoise Cadmium line in an external magnetic field
- Investigation of the polarization of the quartet and sextet components

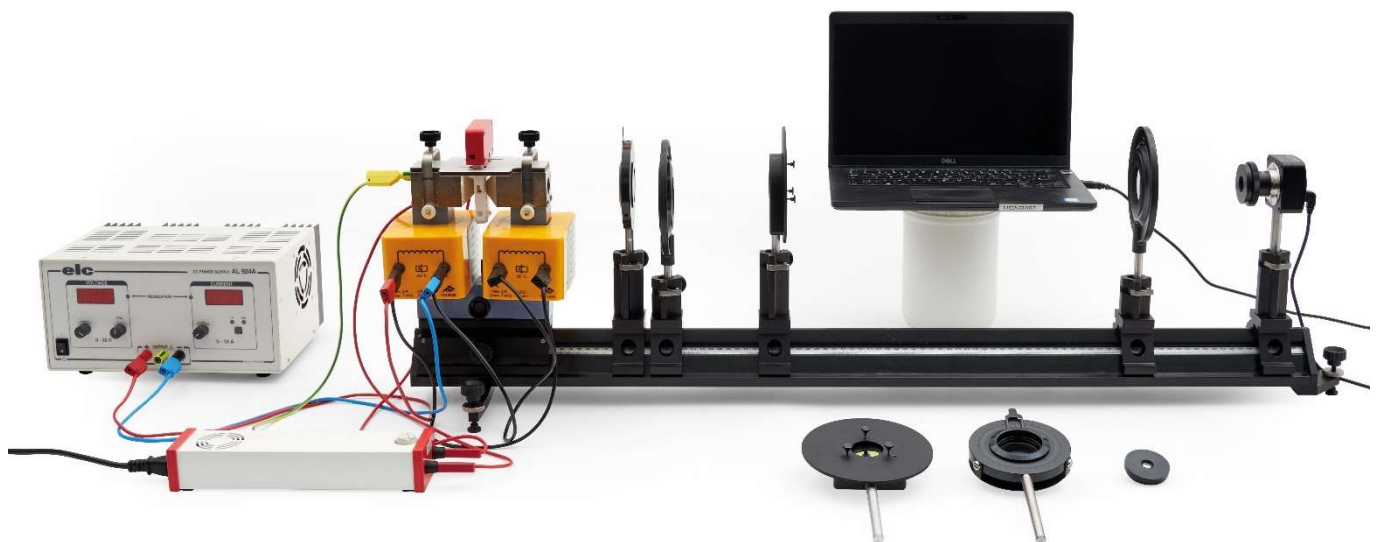


Fig. 1: Experimental setup for the anomalous Zeeman effect in longitudinal configuration

GENERAL PRINCIPLES

The Zeeman effect refers to the splitting of atomic energy levels or spectral lines under the influence of an external magnetic field. It was discovered in 1896 by its namesake Pieter Zeeman as a broadening of the sodium D lines and classically explained by Hendrik Antoon Lorentz with the help of the Lorentz force, which the magnetic field exerts on the electrons in the atomic shell. In this so-called normal Zeeman effect, as is the case for the red cadmium line ($\lambda = 643.8 \text{ nm}$), for example, a double splitting into a line doublet is observed parallel to the magnetic field (longitudinal) and a triple splitting into a line triplet is observed perpendicular to the magnetic field (transversal). More complex splittings are referred to as the anomalous Zeeman effect, which could only be explained with the help of the existence of the electron spin postulated by Goudsmit and Uhlenbeck in 1925. Quantum mechanically, the anomalous Zeeman effect is based on the interaction of the magnetic field with the magnetic moment of the electron shell generated by the orbital angular momentum and spin of the electrons. In this respect, the anomalous Zeeman effect represents the normal case, the normal Zeeman effect a special case.

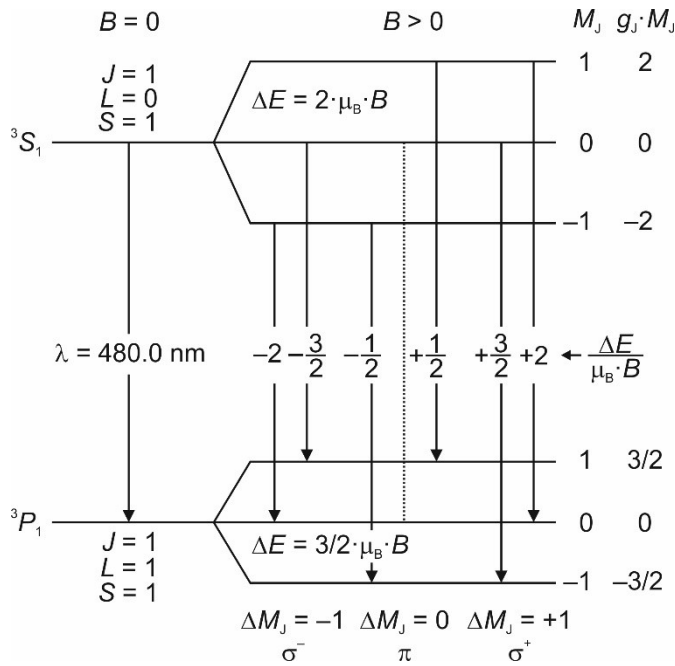


Fig. 2: Anomalous Zeeman effect at the turquoise cadmium spectral line. Splitting of the energy levels and transitions permitted according to the selection rules for electric dipole radiation

Hyperfine structure splitting

Even without an external magnetic field, additional lines can be observed, which are referred to as hyperfine structure. This is caused by the fact that the Cd lamp not only contains the isotope ¹¹⁴Cd with nuclear spin 0 (isotope ratio 28.7%), but also the isotopes ¹¹¹Cd (12.8%) and ¹¹³Cd (12.2%) with nuclear spin 1/2, with which the electrons interact. This results in four additional lines that are shifted by $\Delta\lambda = -0.0078 \text{ nm}$, -0.0029 nm , $+0.0061 \text{ nm}$ and $+0.0014 \text{ nm}$ compared to the turquoise Cd line. The first three lines can be resolved and observed in the experiment, the fourth line and the turquoise Cd line are too close to each other.

Anomalous Zeeman effect

The anomalous Zeeman effect occurs for transitions between atomic states with total spin $S \neq 0$. The turquoise Cd line corresponds to the transition ${}^3S_1 \rightarrow {}^3P_1$ with the wavelength $\lambda = 480.0 \text{ nm}$ (Fig. 2). Since both levels have a total spin with the quantum number $S = 1$, the anomalous Zeeman effect can be observed here. In the case of Cd, LS coupling is present in the outer shells, as the inner electrons shield the outer electrons from the nucleus. The total angular momentum $\mathbf{J} = \mathbf{L} + \mathbf{S}$ generates a magnetic moment

$$(1) \quad \boldsymbol{\mu} = \boldsymbol{\mu}_L + \boldsymbol{\mu}_S = \frac{\mu_B}{\hbar} \cdot (g_L \cdot \mathbf{L} + g_S \cdot \mathbf{S})$$

with the Bohr Magneton

$$(2) \quad \mu_B = \frac{e}{2 \cdot m_e} \cdot \hbar = 9.274 \cdot 10^{-24} \frac{\text{J}}{\text{T}}$$

e : elementary charge
 m_e : mass of the electron
 $\hbar = \hbar/2\pi$: reduced Planck constant

and $g_L = 1$, $g_S = 2$ for an electron. Because of $g_L \neq g_S$, \mathbf{J} and $\boldsymbol{\mu}$ are not parallel. Only the component

$$(3) \quad \boldsymbol{\mu}_J = g_J \cdot \frac{\mu_B}{\hbar} \cdot \mathbf{J}$$

of $\boldsymbol{\mu}$ parallel to \mathbf{J} provides a contribution ΔE , where g_J is given by the Landé equation

$$(4) \quad g_J = 1 + \frac{J(J+1) - L(L+1) + S(S+1)}{2J(J+1)}$$

with the quantum numbers J for the total angular momentum, L for the total orbital angular momentum and S for the total spin.

In an external magnetic field

$$(5) \quad \mathbf{B} = \begin{pmatrix} 0 \\ 0 \\ B \end{pmatrix}$$

the energy

$$(6) \quad E = \boldsymbol{\mu}_J \cdot \mathbf{B} = \mu_{J,z} \cdot B$$

is associated with the magnetic moment. Due to the directional quantization, the component J_z of the total angular momentum parallel to the magnetic field can only have the values

$$(7) \quad J_z = M_J \cdot \hbar \text{ with } M_J = -J, -(J-1), \dots, (J-1), J$$

The energy level with the total angular momentum quantum number J thus splits into $2J+1$ equidistant components, which differ in the magnetic quantum number M_J (Fig. 2). With Eq. (3) follows

$$(8) \quad \mu_{J,z} = g_J \cdot \frac{\mu_B}{\hbar} \cdot J_z$$

thus, according to Eq. (6)

$$(9) \quad E = \mu_{J,z} \cdot B = g_J \cdot \frac{\mu_B}{\hbar} \cdot J_z \cdot B$$

and finally with Eq. (7):

$$(10) \quad E = g_J \cdot M_J \cdot \mu_B \cdot B$$

The energy difference between two levels with energies E_1 and E_2 ($E_1 > E_2$) is therefore calculated as follows:

$$(11) \quad \Delta E = E_1 - E_2 = (g_{J,1} \cdot M_{J,1} - g_{J,2} \cdot M_{J,2}) \cdot \mu_B \cdot B$$

According to Eq. (7), both levels 3S_1 and 3P_1 are split into three components, each with the equidistant energy difference given by Eq. (11).

According to the selection rules for electric dipole radiation, transitions between these levels are permitted with

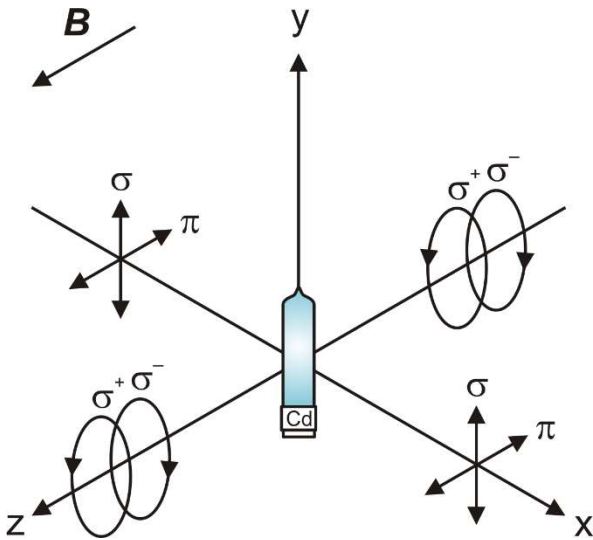


Fig. 3: Polarization of electric dipole radiation depending on the direction of propagation

$$(12) \Delta M_J = \begin{cases} +1 & \text{(right circularly polarized light, } \sigma^+) \\ 0 & \text{(linearly polarized light, } \pi) \\ -1 & \text{(left circularly polarized light, } \sigma^-) \end{cases}$$

where the emitted light is polarized as indicated above. An exception are transitions between levels with $M_J = 0$ and $\Delta J = 0$, which are forbidden (Fig. 2, dashed line).

According to $E = \hbar \cdot \omega$, a total of six spectral lines shifted by

$$(13) \Delta\lambda = -\frac{\lambda^2}{2 \cdot \pi \cdot \hbar \cdot c} \cdot \Delta E$$

c: vacuum speed of light

can be observed, two π components and four σ components with a correspondingly higher or lower wavelength. For the smallest energy difference $|\Delta E| = \frac{1}{2} \cdot \mu_B \cdot B$ (Fig. 2), a shift of $|\Delta\lambda| = 0,0023 \text{ nm}$ results from equation (13) by inserting equations (11) and (2) for the flux density $B = 422 \text{ mT}$ set in the experiment.

The spatial distribution of the emitted light is different for the π and the σ components. The case $\Delta M_J = 0$ classically corresponds to a Hertzian dipole oscillating parallel to the magnetic field. Accordingly, linearly polarized light is emitted perpendicular to the magnetic field (transversal) and no light is emitted parallel to the magnetic field (longitudinal) (Fig. 3). The cases $\Delta M_J = \pm 1$ correspond to two dipoles oscillating perpendicular to each other with a phase difference of 90° . Accordingly, light that is circularly polarized parallel to the magnetic field is emitted both parallel and perpendicular to the magnetic field, namely left circularly polarized for $\Delta M_J = -1$ and right circularly polarized for $\Delta M_J = +1$.

A quarter-wavelength filter with a downstream polarization filter is therefore required to analyze the polarization of light when observing in the longitudinal direction, as the observation is made perpendicular to the polarization plane of the σ components (Fig. 3). The quarter-wavelength filter converts the circularly polarized light into linearly polarized light, which can then be analyzed using the polarization filter. When the quarter-wavelength filter is set to -45° , the σ^+ components are con-

verted accordingly and can be observed, while the σ^- components disappear. When the quarter-wavelength filter is set to $+45^\circ$, the opposite is true. Only one polarization filter is required for observation in the transverse direction, as the observation is made parallel to the plane of polarization of the σ components, and these appear therefore linearly polarized (Fig. 3). The π components are always linearly polarized. When the polarization filter is set to 0° , the σ components can be observed accordingly, while the π components disappear. When the polarization filter is set to 90° , the opposite is true.

In the experiment, the splitting is observed with the help of a digital camera preceded by a Fabry-Pérot etalon and imaging optics. The Fabry-Pérot etalon is designed to fulfill the resonance condition for the specific wavelength of 480.0 nm of the turquoise Cd line. When the light from the cadmium lamp passes through the Fabry-Pérot etalon, interference rings are created which, like the spectral line, are split as a function of the external magnetic field and imaged onto the camera sensor by the optics. Observation parallel or perpendicular to the external magnetic field is made possible by a rotating electromagnet. The splitting is observed qualitatively and the polarization of the quartet and sextet components is examined using a quarter-wavelength filter with polarization attachment and a polarization filter.

EQUIPMENT LIST

1	Cadmium lamp with accessories @230 V	1021366
or		
1	Cadmium lamp with accessories @115 V	1021747
1	Fabry-Pérot etalon 480 nm	1025375
1	DC power supply, linear regulated, 1 – 30V, 0 – 10A @230V	1025380
or		
1	DC power supply, 0 – 20 V, 0 – 5 A @115 V	1003311
1	U Core D	1000979
2	Coil D, 900 turns	1012859
1	Electromagnet accessory for Zeeman effect	1021365
1	Microscope camera BRESSER MikroCam SP 3.1	1024060
1	Lens 12 mm for Bresser microscope camera	1024059
1	Stainless steel rod with 1/4 inch thread, 100 mm	1025431
1	Bandpass interference filter, 480nm	1025377
2	Convex lens on stem f =+100 mm	1003023
1	Quarter-wavelength filter on stem	1021353
1	Polarising attachment	1021364
1	Polarisation filter on stem	1008668
1	Optical precision bench D, 1000 mm	1002628
1	Support for optical bench D, set	1012399
1	Optical base D	1009733
3	Optical rider D, 90/36	1012401
2	Optical rider D, 60/36	1002639
1	Safety experiment leads, 75 cm, blue, red, (2 pcs)	1017718
1	Safety experiment leads, 75 cm, black, (2 pcs)	1002849

SETUP AND SAFETY INSTRUCTIONS

The procedure of this experiment requires that the assembly of the components as well as the experimental setup and adjustment have been carried out according to the instructions for the experiment on the normal Zeeman effect, considering all the safety instructions formulated therein. Instead of the Fabry-Pérot etalon and the color filter for the red Cd line, the Fabry-Pérot etalon 480 nm (1025375) and the bandpass interference filter 480 nm (1025377) are to be used.

The maximum current through the coils D with 900 turns is 5 A (7 minutes). It can be doubled for short periods (30 seconds). The coils have an internal reversible thermal fuse which trips at a winding temperature of 85°C. The reset time is 10-20 minutes, depending on the ambient temperature.

- Carry out the measurement quickly enough to prevent the thermal fuse from tripping due to high currents flowing for too long.
- Do not operate the coils without a transformer core.

GENERAL NOTES

The camera software must be installed on the measuring computer.

It is recommended to carry out the experiment in a dark room in order to minimize stray light from the surroundings and to achieve optimum exposure and contrast of the camera's live image.

Due to the temperature sensitivity of Fabry-Pérot etalons, the center of the interference rings may look differently depending on the ambient temperature and may therefore differ from the screenshots in this manual.

The turquoise, which corresponds to the wavelength of 480 nm, cannot be displayed in the RGB color space of the camera and therefore appears blue.

EXPERIMENT PROCEDURE, MEASUREMENT EXAMPLE AND EVALUATION

Observation in longitudinal direction

Carry out the following steps, observe how the interference rings change and take screenshots (Fig. 4).

- Do not apply an external magnetic field.

Only the interference rings generated by the Fabry-Pérot etalon are observed, each of which corresponds to the turquoise Cd spectral line, as well as other interference rings that correspond to the spectral lines of the hyperfine structure (Fig. 4a).

Note:

In order to be able to identify the hyperfine structure optimally, it is recommended to overexpose the interference rings of the turquoise Cd line, i.e. to set a correspondingly longer exposure time.

- Apply an external magnetic field by switching on the DC power supply unit and increasing the current through the coils to 4.5 A ($B = 422$ mT).

Notes:

When a magnetic field is applied, the exposure time should be ≥ 20 ms, as otherwise "flickering lines" may occur due to an interference of the camera's "rolling shutter sensor". As the interference rings of the hyperfine structure affect the observation of the anomalous Zeeman effect, it is recommended to set a correspondingly shorter exposure time.

The fourfold splitting into the two σ^- and the two σ^+ components is observed, the two π components are not observed (Fig. 4b).

- With the magnetic field applied, position the quarter-wavelength filter with polarization attachment between the electromagnet and the condenser lens using a long optical rider (1012401).

Note:

The quarter-wavelength filter must be on the side of the Cd lamp.

- With the magnetic field applied, set the quarter-wavelength filter with polarization attachment to -45° .

The two σ^- components disappear (Fig. 4c).

- With the magnetic field applied, set the quarter-wavelength filter with polarization attachment to $+45^\circ$.

The two σ^+ components disappear (Fig. 4d).

- Remove the quarter-wavelength filter with polarization attachment from the beam path.
- Reduce the current to zero and switch off the DC power supply unit.

Observation in transversal direction

- Turn the electromagnet so that the pole pieces are oriented perpendicular to the direction of the optical axis.
- Do not apply an external magnetic field.

Only the interference rings generated by the Fabry-Pérot etalon are observed, each of which corresponds to the turquoise Cd spectral line, as well as other interference rings that correspond to the spectral lines of the hyperfine structure (Fig. 4e, Fig. 5).

- Apply an external magnetic field by switching on the DC power supply unit and increasing the current through the coils to 4.5 A ($B = 422$ mT).

The sixfold splitting into the two π , the two σ^- and the two σ^+ components is observed (Fig. 4f, Fig. 6).

- With the magnetic field applied, position the polarization filter between the electromagnet and the condenser lens and set it to 0° , i.e. perpendicular to the magnetic field.

The two π components disappear (Fig. 4g, Fig. 6).

- With the magnetic field applied, set the polarization filter to 90° , i.e. parallel to the magnetic field.

The two σ^- and the two σ^+ components disappear (Fig. 4h, Fig. 6).

- Remove the polarization filter from the beam path.
- Reduce the current to zero and switch off the DC power supply unit.

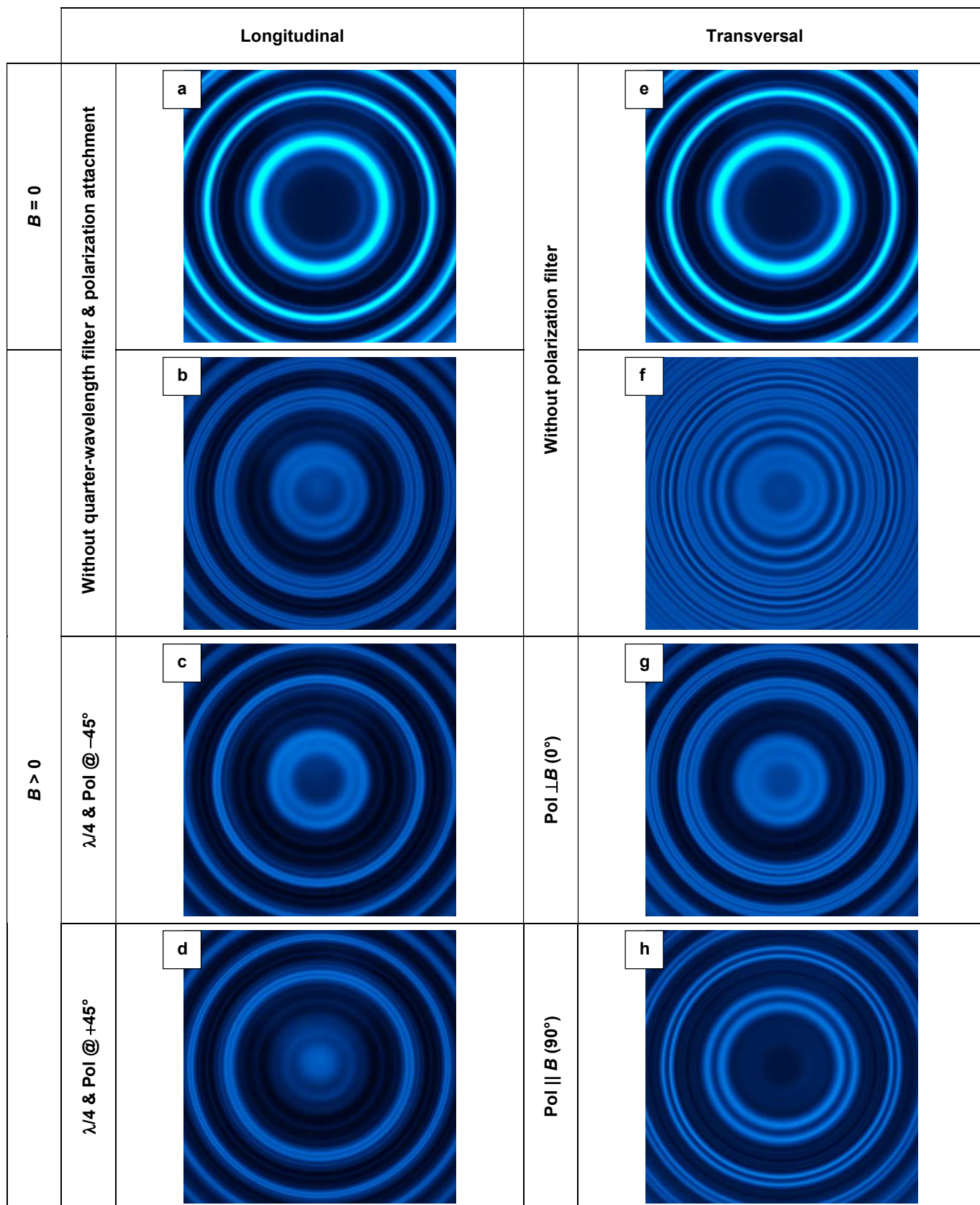


Fig. 4: Observation of the fourfold and sixfold splitting of the turquoise cadmium line in the external magnetic field and investigation of the polarization

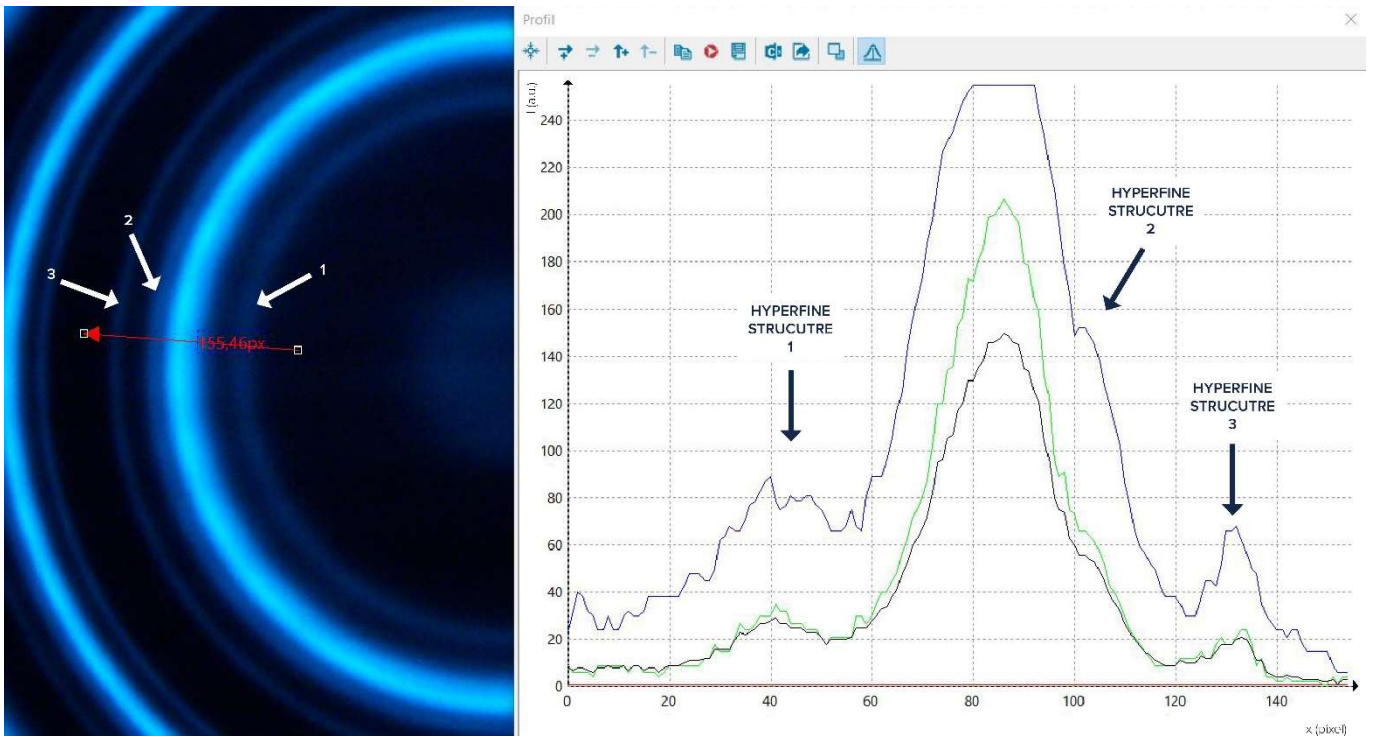


Fig. 5: Hyperfine structure splitting (left) and brightness profile (right, black curve) along the drawn arrow. Red, green and blue curve: Brightness profile of the red, green and blue color channel. The lines shifted by $\Delta\lambda = -0,0078 \text{ nm}$ (3) and $+0,0061 \text{ nm}$ (1) are clearly visible, the line shifted by $-0,0029 \text{ nm}$ (2) can be recognized as a shoulder. The line shifted by $+0,0014 \text{ nm}$ is so close to the turquoise Cd line that it cannot be resolved and therefore cannot be observed

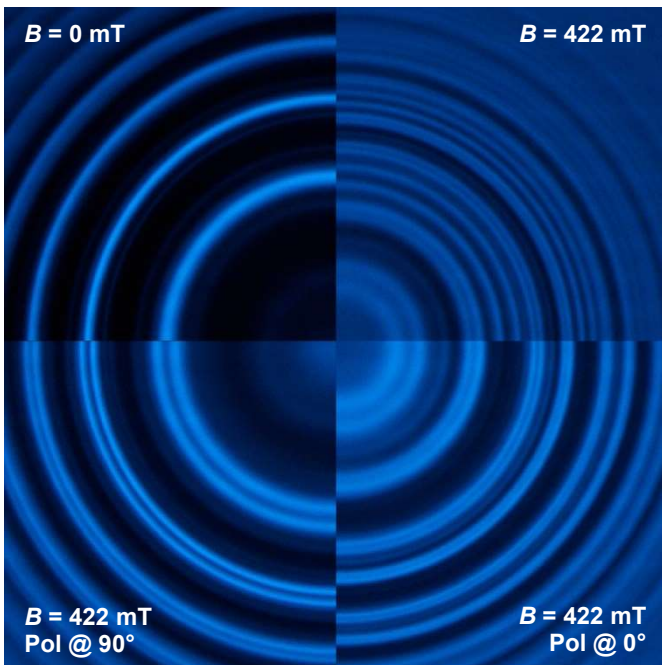


Fig. 6: Anomalous Zeeman effect when observed in transversal direction. Splitting of the interference rings and polarization states at a glance

Fabry-Pérot Interferometer, Determination of the Bohr Magneton

SPECTROSCOPY WITH A FABRY-PÉROT ETALON

- Experimental introduction to the Fabry-Pérot interferometer using the example of the normal Zeeman effect
- Measuring the interference rings of the Fabry-Pérot etalon as a function of the external magnetic field
- Determination of the Bohr Magneton

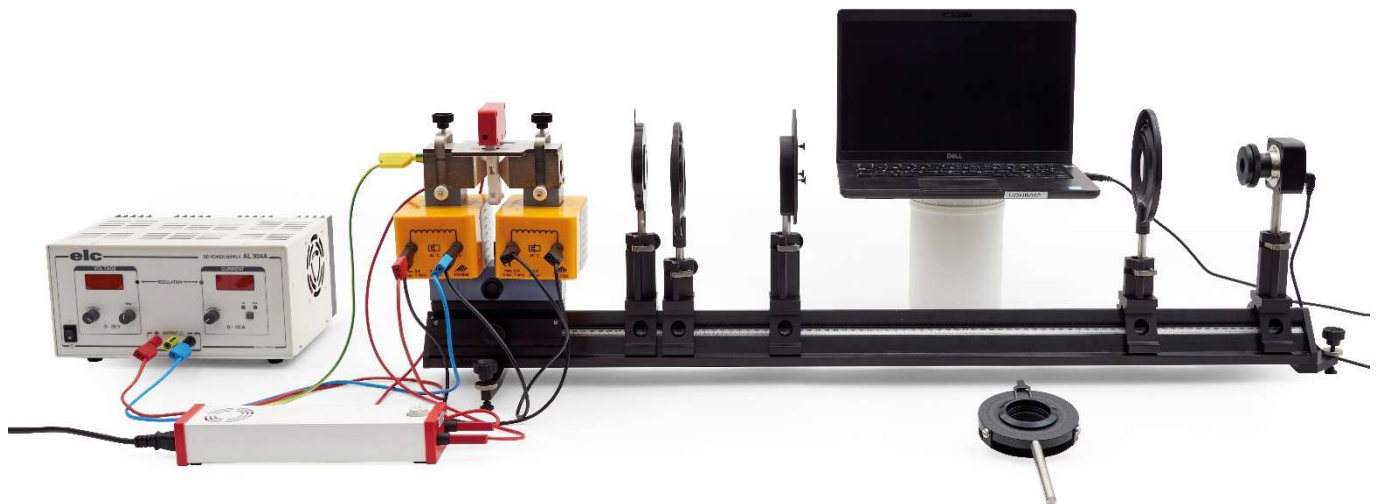


Fig. 1: Experimental setup for the normal Zeeman effect in longitudinal configuration

GENERAL PRINCIPLES

The Fabry-Pérot interferometer, developed by its namesakes Charles Fabry and Alfred Pérot, is an optical resonator consisting of two semi-transparent mirrors. A Fabry-Pérot interferometer with a fixed distance between the mirrors is known as a Fabry-Pérot etalon. As it is designed to fulfill the resonance condition for a specific wavelength, the etalon also acts as an optical filter. An incident light beam is reflected several times in the etalon so that the light beams transmitted with each reflection interfere with each other. This multi-beam interference produces an intensity distribution in transmission with narrow maxima and broad minima. Together with the high interference order at correspondingly large resonator dimensions, this results in a high optical quality and correspondingly high resolution. This means that small spectral splittings, such as those present in the normal Zeeman effect at the red Cd line ($\lambda = 643.8 \text{ nm}$, $\Delta\lambda = 0.0068 \text{ nm}$ at $B = 350 \text{ mT}$), can be resolved.

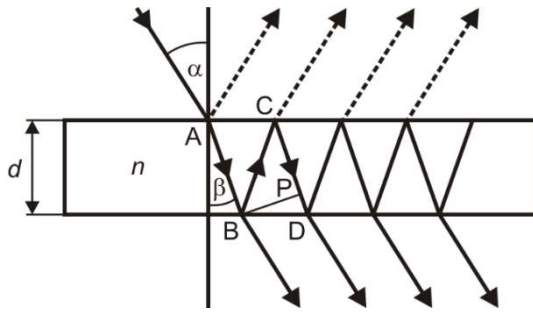


Fig. 2: Beam path in the Fabry-Pérot etalon

The focus of this experiment is on spectroscopy with a Fabry-Pérot etalon. The Fabry-Pérot etalon is positioned in front of the camera together with imaging optics, which is used to observe Zeeman splitting. When the light from the cadmium lamp passes through the Fabry-Pérot etalon, interference rings are created which, like the spectral line, split depending on the external magnetic field and are imaged onto the camera by the optics. Observation parallel or perpendicular to the external magnetic field is made possible by a rotating electromagnet.

The Fabry-Pérot etalon consists of a quartz glass plate with a semi-reflective mirror coating of high reflectivity on both sides (Fig. 2). In this case, the etalon is designed in such a way that the resonance condition for the wavelength $\lambda = 643,8 \text{ nm}$ of the red Cd line is fulfilled. In this sense, the etalon also acts as an optical filter. The thickness d , the refractive index n and the reflection coefficient R of the etalon are as follows:

- $d = 4 \text{ mm}$
- (1) $n = 1.4567$
- $R = 0.85$

An incident light beam is reflected several times in the etalon. The light beams transmitted during each reflection interfere with each other. The path difference Δs between two neighboring transmitted light beams, e.g. the light beams emerging at points B and D in Fig. 2, is:

$$(2) \Delta s = n \cdot (\overline{BC} + \overline{CP}).$$

From

$$(3) \overline{CP} = \overline{BC} \cdot \cos(2 \cdot \beta),$$

$$(4) d = \overline{BC} \cdot \cos(\beta),$$

Snellius' law of refraction ($n_{\text{air}} \approx 1$)

$$(5) \sin(\alpha) = n \cdot \sin(\beta)$$

and the addition theorems

$$(6) \begin{aligned} \cos(\beta) &= \sqrt{1 - \sin^2(\beta)} \\ \cos(2 \cdot \beta) &= 1 - 2 \cdot \sin^2(\beta) \end{aligned}$$

the path difference results in

$$(7) \Delta s = 2 \cdot d \cdot \sqrt{n^2 - \sin^2(\alpha)} = 2 \cdot d \cdot n \cdot \cos(\beta)$$

and from this, the condition for the existence of interference maxima:

$$(8) k \cdot \lambda = 2 \cdot d \cdot \sqrt{n^2 - \sin^2(\alpha_k)} = 2 \cdot d \cdot n \cdot \cos(\beta_k).$$

k : Whole number, interference order

α_k : Incidence angle of the k th interference order

β_k : Refraction angle of the k th interference order

Overall, an interference pattern of concentric rings is generated. The refraction at the boundary surfaces of the glass plate of the Fabry-Pérot etalon can be neglected as it only shifts the interference pattern in parallel. Therefore, the refraction angle β is replaced by the incidence angle α , and the interference condition (8) results in

$$(9) k \cdot \lambda = 2 \cdot d \cdot n \cdot \cos(\alpha_k) \approx 2 \cdot d \cdot n \cdot \left(1 - \frac{\alpha_k^2}{2}\right),$$

with the expansion $\cos(x) \approx (1 - x^2 / 2)$ of the cosine function.

The interference pattern is imaged onto the camera using a convex lens (Fig. 3). The following relationship exists between the angle α_k at which the k th order interference ring appears, the radius r_k of the k th order interference ring and the focal length f of the lens (Fig. 3):

$$(10) r_k = f \cdot \tan(\alpha_k) \approx f \cdot \alpha_k,$$

with the small angle approximation $\tan(x) \approx x$. From equation (9) follows for the interference order k and the angle α_k

$$(11) k = k_0 \cdot \cos(\alpha_k) \approx k_0 \cdot \left(1 - \frac{\alpha_k^2}{2}\right) \text{ with } k_0 = \frac{2 \cdot d \cdot n}{\lambda}$$

and

$$(12) \alpha_k = \sqrt{\frac{2 \cdot (k_0 - k)}{k_0}}.$$

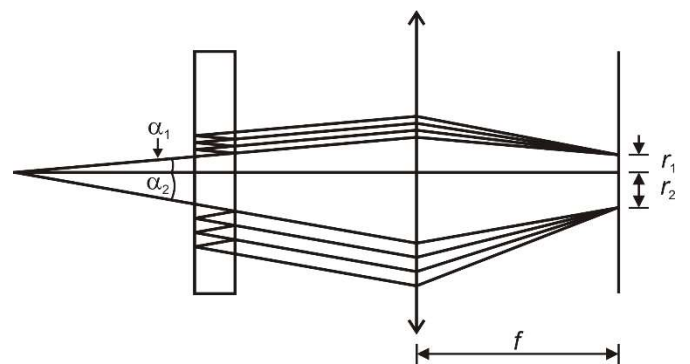


Fig. 3: Imaging the interference rings of the Fabry-Pérot etalon onto the digital camera

According to equation (11), because of $|\cos(\alpha_k)| \leq 1$, the interference order k is maximum for $\alpha_k = 0$, i.e. in the center of the interference rings, and corresponds to the parameter k_0 , which is generally not a whole number. Since the interference rings are counted from the center in the experiment, the interference order k is indexed with a whole number j , which identifies the k th interference order with the j th interference ring counted from the center, in generalization of the parameter k_0 already introduced.

The first bright interference ring with order k_1 appears according to equation (12) at the angle

$$(13) \alpha_{k_1} = \sqrt{\frac{2 \cdot (k_0 - k_1)}{k_0}},$$

where k_1 is the next whole number that is smaller than k_0 . As k_0 is generally not a whole number, the difference $k_0 - k_1$ is less than 1. Therefore, a parameter ε is defined as follows:

$$(14) \varepsilon = k_0 - k_1 \text{ with } 0 < \varepsilon < 1$$

For all interference rings with $j \geq 2$, the order number k_j is decreased by 1 in each case, so that for the interference order of the j th interference ring counted from the center the following is generally true:

$$(15) k_j = (k_0 - \varepsilon) - (j - 1)$$

For $j = 1$, equation (15) just corresponds to the definition of ε from equation (14). Substituting equations (12) (with $k = k_j$) and (15) into equation (10) results in

$$(16) r_j = \sqrt{\frac{2 \cdot f^2}{k_0} \cdot \sqrt{(j-1) + \varepsilon}},$$

where, for the sake of simplicity, $r_{k_j} \rightarrow r_j$ was set for indexing without restriction of generality. This convention is retained in the following. It follows from equation (16) that the difference between the radius squares of neighboring interference rings is constant:

$$(17) r_{j+1}^2 - r_j^2 = \frac{2 \cdot f^2}{k_0} = \text{const.}$$

From equations (16) and (17) follows:

$$(18) \varepsilon = \frac{r_{j+1}^2}{r_{j+1}^2 - r_j^2} - j.$$

If the interference rings are split into two very closely spaced components a and b , whose wavelengths differ only slightly from each other, for the first interference ring counted from the center, for example, follows from equation (14):

$$(19) \begin{aligned} \varepsilon_a &= k_{0,a} - k_{1,a} = \frac{2 \cdot d \cdot n}{\lambda_a} - k_{1,a} \\ \varepsilon_b &= k_{0,b} - k_{1,b} = \frac{2 \cdot d \cdot n}{\lambda_b} - k_{1,b} \end{aligned}$$

Since the two components belong to the same interference order, and provided that the interference rings do not overlap by more than one whole order, $k_{1,a} = k_{1,b}$ and thus:

$$(20) \varepsilon_a - \varepsilon_b = k_{0,a} - k_{0,b} = 2 \cdot d \cdot n \cdot \left(\frac{1}{\lambda_a} - \frac{1}{\lambda_b} \right).$$

Equation (20) does not explicitly depend on the interference order. If equation (18) is formulated for both components a and b and inserted into equation (20), the following results:

$$(21) \left(\frac{1}{\lambda_a} - \frac{1}{\lambda_b} \right) = \frac{1}{2 \cdot d \cdot n} \cdot \left(\frac{r_{j+1,a}^2}{r_{j+1,a}^2 - r_{j,a}^2} - \frac{r_{j+1,b}^2}{r_{j+1,b}^2 - r_{j,b}^2} \right).$$

From equation (17) it follows that the difference of the radius squares of the component a or b for neighboring interference orders j and $j+1$ with $j > 0$ due to $\lambda_a \approx \lambda_b$ and thus $k_{0,a} \approx k_{0,b}$ are approximately equal:

$$(22) \Delta_a^{j+1,j} = r_{j+1,a}^2 - r_{j,a}^2 = r_{j+1,b}^2 - r_{j,b}^2 = \Delta_b^{j+1,j}.$$

Accordingly, the following applies for two components a and b of the same interference order j with $j > 0$:

$$(23) \delta_{a,b}^j = r_{j,a}^2 - r_{j,b}^2 = r_{j+1,a}^2 - r_{j+1,b}^2 = \delta_{a,b}^{j+1}.$$

Substituting equations (22) and (23) into equation (21) results in:

$$(24) \left(\frac{1}{\lambda_a} - \frac{1}{\lambda_b} \right) = \frac{1}{2 \cdot d \cdot n} \cdot \frac{\delta_{a,b}^{j+1}}{\Delta_a^{j+1,j}} \text{ for all } j > 0$$

Since equation (22) applies to both components a and b of neighboring interference rings and equation (23) applies to all interference rings, mean values

$$(25) \delta = \overline{\delta_{a,b}^j}$$

and

$$(26) \Delta = \overline{\Delta_a^{j+1,j}}$$

can be calculated and inserted into equation (24):

$$(27) \left(\frac{1}{\lambda_a} - \frac{1}{\lambda_b} \right) = \frac{1}{2 \cdot d \cdot n} \cdot \frac{\delta}{\Delta}.$$

With

$$(28) \Delta E_{a,b} = h \cdot c \cdot \left(\frac{1}{\lambda_a} - \frac{1}{\lambda_b} \right) = \mu_B \cdot B$$

follows from equation (27):

$$(29) \frac{\delta}{\Delta} = 2 \cdot \frac{d \cdot n}{h \cdot c} \cdot \mu_B \cdot B = a \cdot B \text{ with } a = 2 \cdot \frac{d \cdot n}{h \cdot c} \cdot \mu_B.$$

The ratio δ / Δ can be measured as a function of the magnetic flux density B , plotted graphically, and the Bohr magneton μ_B can be determined from the slope a of a linear fit.

EQUIPMENT LIST

1	Cadmium lamp with accessories @230 V	1021366
or		
1	Cadmium lamp with accessories @115 V	1021747
1	Fabry-Pérot etalon 644 nm	1020903
1	DC power supply, linear regulated, 1 – 30V, 0 – 10A @230V	1025380
or		
1	DC power supply, 0 – 20 V, 0 – 5 A @115 V	1003311
1	U Core D	1000979
2	Coil D, 900 turns	1012859
1	Electromagnet accessory for Zeeman effect	1021365
1	Microscope camera BRESSER MikroCam SP 3.1	1024060
1	Lens 12 mm for Bresser microscope camera	1024059
1	Stainless steel rod with ¼ inch thread, 100 mm	1025431
1	Red filter mounted on holder	1025376
2	Convex lens on stem $f = +100$ mm	1003023
1	Quarter-wavelength filter on stem	1021353
1	Polarising attachment	1021364
1	Polarisation filter on stem	1008668
1	Optical precision bench D, 1000 mm	1002628
1	Support for optical bench D, set	1012399
1	Optical base D	1009733
3	Optical rider D, 90/36	1012401
2	Optical rider D, 60/36	1002639
1	Safety experiment leads, 75 cm, blue, red, (2 pcs)	1017718
1	Safety experiment leads, 75 cm, black, (2 pcs)	1002849

SETUP AND SAFETY INSTRUCTIONS

The procedure of this experiment requires that the assembly of the components as well as the experimental setup and adjustment have been carried out according to the instructions for the experiment on the normal Zeeman effect, considering all the safety instructions formulated therein.

The maximum current through the coils D with 900 turns is 5 A (7 minutes). It can be doubled for short periods (30 seconds). The coils have an internal reversible thermal fuse which trips at a winding temperature of 85°C. The reset time is 10-20 minutes, depending on the ambient temperature.

- Carry out the measurement quickly enough to prevent the thermal fuse from tripping due to high currents flowing for too long.
- Do not operate the coils without a transformer core.

EXPERIMENT PROCEDURE

Measurement

- Establish the transversal configuration by rotating the electromagnet as described in the instruction manual for the experiment on the normal Zeeman effect.

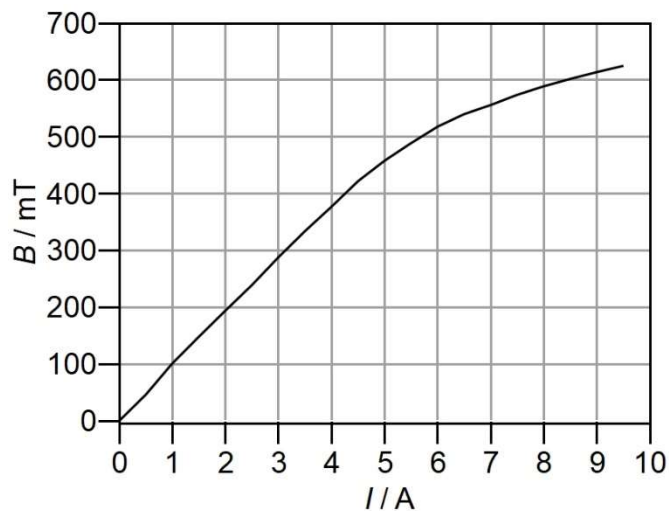


Fig. 4: Calibration curve of the electromagnet

- Focus the 12 mm lens so that the three interference rings of the innermost order, for which they appear clearly separated from each other, are in focus. Do not move the convex lenses (imaging and condenser lens) and do not refocus the 12 mm lens, otherwise the evaluation will give incorrect results.

Note:

Due to the temperature sensitivity of Fabry-Pérot etalons, the center of the interference rings may look differently depending on the ambient temperature and may therefore differ from the screenshots in this manual.

- Switch on the DC power supply unit, increase the current through the coils first to 3 A, then in 0.5 A steps to 5 A and in 1 A steps to 9 A. At each step, take a screenshot ("snapshot") with the camera software and save it as a "JPEG".

Note:

When increasing the current, make sure that the interference rings do not overlap by more than one whole order.

Calibration of the electromagnet

The values for the magnetic flux densities B , which correspond to the set currents I , can be taken from the calibration curve in Fig. 4 or Tab. 1. Alternatively, the calibration curve can be measured as follows:

- Remove the Cd lamp on the housing from the base plate.
- Place a teslameter in the air gap between the two pole pieces (approx. 10 mm) so that the magnetic field sensor is centered.
- Switch on the DC power supply unit and increase the current I through the coils in 0.5 A steps. At each step, measure the values for the magnetic flux density B , note them and plot them against the set currents.
- Reduce the current to zero and switch off the DC power supply unit.
- Insert the Cd lamp back into the base plate.

Tab 1: Calibration of the electromagnet. Set currents I and measured magnetic flux densities B

I / A	B / mT	I / A	B / mT
0.0	0	5.0	458
0.5	46	5.5	489
1.0	101	6.0	518
1.5	148	6.5	540
2.0	194	7.0	556
2.5	239	7.5	574
3.0	288	8.0	589
3.5	334	8.5	602
4.0	377	9.0	614
4.5	422	9.5	625

MEASUREMENT EXAMPLE AND EVALUATION

The following steps are to be carried out for each saved screenshot:

- Open a screenshot in the camera software (click on “File” in the menu bar and select “Open image”).
- Click on “Options” in the menu bar, then on “Measurement”, select “Length Unit” in the window that opens, tick “Pixel” under “Current” and confirm the setting by clicking on “OK”.
- Click on the “Circle” button in the tool bar and select “3 Points”. Place a circle on the innermost interference ring. This is referred to as “C1” in the following.

The “Measurement” window opens automatically.



Fig. 5: Triplet splitting of the red cadmium line ($I = 5.0 A \triangleq B = 458 mT$). Interference rings marked with circles to determine the enclosed areas

- If necessary, adjust the appearance under “Appearance” (e.g. line width/color, show/hide label type).
- Under “Geometry”, note the numerical value for the area in pixels (Tab. 2). Mark further interference rings in the same way (C2-C9, Fig. 5) and note the areas (Tab. 2). Click on the “Track” button (hand symbol) to complete the process.
- Click on “Layer” in the menu bar, select “Merge to image” and click on “OK”.
- Click on “File” in the menu bar, select “Save as” and save the image as a JPEG with a meaningful name.

Note:

The unit of the area is irrelevant for further evaluation, as only relative values and ratios are calculated, not absolute values. The absolute values of the areas (Tab. 2) can deviate significantly depending on the position of the optics.

- Calculate the area differences Δ of the corresponding components of neighboring interference orders (Eq. (22), Tab. 3; circles C4↔C1, C5↔C2, C6↔C3, C7↔C4, C8↔C5, C9↔C6).
- Calculate the area differences δ of neighboring components of the same interference orders (Eq. (23), Tab. 4; circles C2↔C1, C3↔C2, C5↔C4, C6↔C5, C8↔C7, C9↔C8).
- Calculate the mean values from all area differences in Tab. 3 and 4 (Eq. (25), (26)) and enter it in the tables.
- Calculate the ratio δ / Δ of the mean values for all set currents or magnetic flux densities, respectively (Tab. 5). Take the corresponding values for the magnetic flux density from the calibration curve of the electromagnet (Fig. 4, Tab. 1).
- Plot the ratio δ / Δ as a function of the magnetic flux density B and fit a straight line through the origin (Fig. 6).

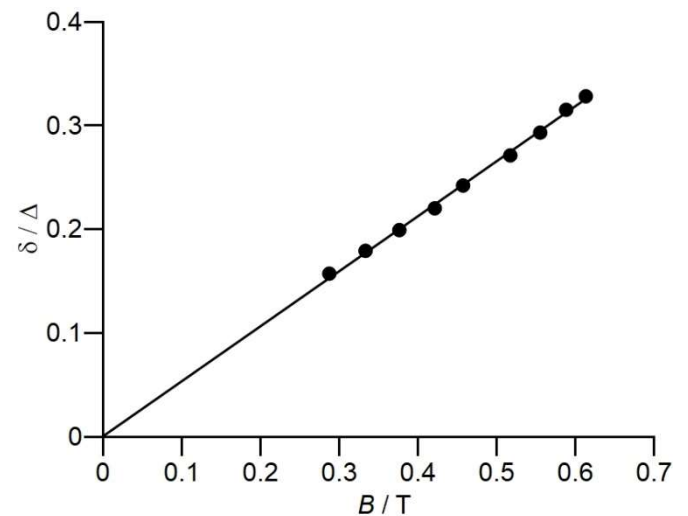


Fig. 6: Ratio δ / Δ of the area differences as a function of the magnetic flux density B . The slope of the fitted straight line through the origin is $a = 0.53 / T$

- Determine the Bohr magneton from the slope $a = 0.53 / T$ The value corresponds to the literature value $9.3 \cdot 10^{-24} \text{ J/T}$ except for approx. 3%
of the fitted straight line using equation (29):

$$\begin{aligned}
 \mu_B &= \frac{1}{2} \cdot \frac{h \cdot c}{d \cdot n} \cdot a \\
 (30) \quad &= \frac{1}{2} \cdot \frac{6.6 \cdot 10^{-34} \text{ Js} \cdot 3.0 \cdot 10^8 \text{ m/s}}{4 \text{ mm} \cdot 1.4567} \cdot 0.53 / T \\
 &= 9.0 \cdot 10^{-24} \frac{\text{J}}{\text{T}}
 \end{aligned}$$

Tab. 2: Areas A enclosed by the interference rings determined with the help of the camera software

I / A	Area A / Pixel								
	C1	C2	C3	C4	C5	C6	C7	C8	C9
3.0	167734	200055	229205	367830	398701	430412	559306	592777	620040
3.5	161486	200196	234474	365742	400854	434853	554225	592457	622683
4.0	157753	199493	238088	358148	398737	439637	552909	592559	624921
4.5	151447	200768	241074	354744	399174	442546	548700	591057	629975
5.0	146500	201657	248223	352695	398436	448720	546544	591877	633671
6.0	140903	199539	254920	345700	400889	451353	539028	591891	637638
7.0	134134	199027	257459	340850	401293	454900	535505	591126	643582
8.0	131146	199745	261665	335577	400627	460375	532289	591173	647816
9.0	130739	200385	265108	332857	398694	463757	531064	590470	651822

Tab. 3: Area differences Δ of the corresponding components of neighboring interference orders

I / A	Area difference Δ / Pixel						Mittelwert
	Δ _{C4,C1}	Δ _{C5,C2}	Δ _{C6,C3}	Δ _{C7,C4}	Δ _{C8,C5}	Δ _{C9,C6}	
3.0	200096	198646	201207	191476	194076	189628	195855
3.5	204256	200658	200379	188483	191603	187830	195535
4.0	200395	199244	201549	194761	193822	185284	195843
4.5	203297	198406	201472	193956	191883	187429	196074
5.0	206195	196779	200497	193849	193441	184951	195952
6.0	204797	201350	196433	193328	191002	186285	195533
7.0	206716	202266	197441	194655	189833	188682	196599
8.0	204431	200882	198710	196712	190546	187441	196454
9.0	202118	198309	198649	198207	191776	188065	196187

Tab. 4: Area differences δ of neighboring components of the same interference orders

I / A	Area difference δ / Pixel						Mean value
	$\delta_{C2,C1}$	$\delta_{C3,C2}$	$\delta_{C5,C4}$	$\delta_{C6,C5}$	$\delta_{C8,C7}$	$\delta_{C9,C8}$	
3.0	32321	29150	30871	31711	33471	27263	30798
3.5	38710	34278	35112	33999	38232	30226	35093
4.0	41740	38595	40589	40900	39650	32362	38973
4.5	49321	40306	44430	43372	42357	38918	43117
5.0	55157	46566	45741	50284	45333	41794	47479
6.0	58636	55381	55189	50464	52863	45747	53047
7.0	64893	58432	60443	53607	55621	52456	57575
8.0	68599	61920	65050	59748	58884	56643	61807
9.0	69646	64723	65837	65063	59406	61352	64338

Tab. 5: Ratio δ / Δ of the area differences for different currents I or magnetic flux densities B , respectively

I / A	B / T	δ / Δ
3.0	0.288	0.157
3.5	0.334	0.179
4.0	0.377	0.199
4.5	0.422	0.220
5.0	0.458	0.242
6.0	0.518	0.271
7.0	0.556	0.293
8.0	0.589	0.315
9.0	0.614	0.328